Acoustic characterization of atmospheric-pressure dielectric barrier discharge plasma jets

Eur. Phys. J. D (2020) xx: xx
https://doi.org/10.1140/epjd/e2020-10203-8

THE EUROPEAN PHYSICAL JOURNAL D

Regular Article

Acoustic characterization of atmospheric-pressure dielectric barrier discharge plasma jets

Vladimir Samara[1], Yvonne Sutton[2], Nicholas Braithwaite[2], and Sylwia Ptasinska[1,3,a]

[1] Radiation Laboratory, University of Notre Dame, Notre Dame, IN 46556, USA
[2] Faculty of Science, Technology, Engineering & Mathematics, The Open University, Milton Keynes MK7 6AA, UK
[3] Department of Physics, University of Notre Dame, Notre Dame, IN 46556, USA

Received 7 April 2020 / Received in final form 14 June 2020
Published online (Inserted Later)

Abstract. In this work, we report the acoustic measurements performed on an atmospheric-pressure plasma jet (APPJ) ignited at various electrical conditions, and attempt to describe the origin of plasma-generated sound waves. The working principle of the APPJ source used for this investigation was based on a DC-pulsed dielectric barrier discharge in a helium flow. Our results indicated that the sound is generated in the plasma core in a glass tube between two cylindrical electrodes, rather than in the plasma jet that extends into the open atmosphere. We also explored the electrical conditions at which the sound level is below 85 dBA; that is, still within the safe level recommended by the National Institute for Occupational Safety and Health. Therefore, our findings can be used to advance our basic and applicable knowledge of APPJs.

1 Introduction

In the last two decades, rapid progress has been made toward understanding the physical phenomena related to atmospheric-pressure plasma jets (APPJs) [1,2]. The main reason for the interest in APPJs is their potential to be used in medical applications such as cancer therapy. Several in vitro and in vivo studies have been conducted in a variety of cancer cell lines that demonstrate the efficacy of atmospheric-pressure plasmas in causing cell death [3]. In addition to these lab-based investigations, there are recent clinical applications of APPJs in which such a source was employed for a growth reduction of neck and head tumor in human patients [4]. The biological interaction between plasma components (photons, electrons, ions, radicals, excited neutrals, and electric and magnetic fields [5,6]) and the treated target can cause significant alterations into cellular components, such as DNA damage [7]; recent research highlights reactive oxygen and nitrogen species as key agents that cause the impairment of cell substructures, DNA alteration and cell death [5,6].

In parallel with this ongoing and intensive research on APPJs' usefulness in patient treatment, and before clinical approval for general use, APPJs will require rigorous safety tests prior to approval for the open market. One significant effect of operating APPJs in the pulsed regime is to generate a significant amount of acoustic sound in the audible range, which can be hazardous to the operator and to the patient during treatment. Therefore, in addition to the safety tests related to the biological effects of plasma and to the safe operation of such devices, one of these tests should also entail the measuring of the sound level.

Sound generation in a plasma has been under investigation periodically since the turn of the last century [8]. It relies on either a forcing mechanism where momentum transfer from charged particles to neutral gas molecules during the collisions results in a forcing effect akin to the front face of a conventional loudspeaker or on a thermal mechanism where pressure fluctuations are caused by rapid expansion within the ionized column in a similar effect to lightning strike. The pressure variation from both mechanisms can be expressed using the ideal gas law as follows:

$$\Delta P = \Delta n_g k T_g + n_g k \Delta T_g$$

where ΔP is the pressure change, $\Delta T_g, T_g$ are the changing and steady-state gas temperature, k is Boltzmann's constant, and $n_g = N/V$ is the number density, where N is the particle number and V is the gas volume. The first term describes an isothermal system where localized density variations result from the ion collisions and reflects the behavior of the forcing mechanism. For the adiabatic system that is described by the second term, the pressure variation results from the changing gas temperature that occurs due to collisions between the high energy electrons and neutral gas components. Changing temperature and density can be achieved through modulation of the electric field and modulation in the audio frequency range will result in audible sound emission.

[a] e-mail: sptasins@nd.edu

There have been many examples of research into plasma "loudspeakers" using both mechanisms but not using APPJs [9–13]. As with other sound generation devices, a commercial APPJ source should also satisfy acoustic safety norms prescribed by the National Institute for Occupational Safety and Health [14]. For example, the dangerous noise level is 85 dBA for continuous exposure over eight hours. Numerous characterizations of APPJs are reported in the literature, which described primarily their electrical, optical, and chemical properties or their biological effects, particularly at the molecular level. Although some scientific reports have described sound generation by other atmospheric pressure plasmas [12,15,16], not many works have been reported on acoustic measurements of APPJs [17]. In this work, we performed a series of acoustic measurements both to assess the safe sound level produced during APPJ operation and to indicate the origin of the sound, which are the characteristics that are important for the applied and fundamental aspects of plasma science, respectively.

2 Experimental set-up

A number of plasma sources have been developed that have different geometries of dielectric barrier coated electrodes through which gas flows, or that involve the application of different voltage waveforms and frequencies to launch an APPJ into the open atmosphere [1,18–20]. In these sources, a plume of gas excited originally inside the dielectric tube in the region between the electrodes is conveyed outwards beyond the source, thereby generating the jet.

The APPJ source in this study consisted of a fused silica tube with inner and outer diameters of 5 mm and 6 mm, respectively, as well as two 50 mm brass electrodes located on the outside of the tube. The distance between the electrodes (distance k) and the distance of the electrode from the tube outlet (distance l) were adjustable, as shown in Figure 1. A detailed description of the entire APPJ source assembly was reported previously [21,22]. The custom-made, high voltage (HV), direct current (DC) pulsed power supply incorporated a push-pull MOSFET switcher by Behlke (HTS 151-03-GSM). The power supply was able to produce either positive or negative voltage pulses by using a positive or negative HV DC power source (EsdEmc DC-DC High Voltage Modules, HVM-A203.13P24 for positive voltage and HVM-A203.13N24 for negative voltage). DC pulses with the amplitude up to 12 kV were applied to the powered electrode that was closer to the tube outlet, at a driving frequency between 10 Hz and 5 kHz; the other electrode was grounded. The pulse duration varied between 10 and 1000 μs. The current was measured and recorded by an induction coil (Pearson Current Monitor Model 2877, Pearson Electronics) at the grounded electrode, and the applied voltage was measured at the powered electrode using an HV probe (Tektronix P6015A). Fast imaging was done by Princeton Instruments Pi-Max ICCD camera. The temperature was measured by an Optocon TS2 GaAs fiber optic temperature sensor [23]. This sensor was made out of an insulator

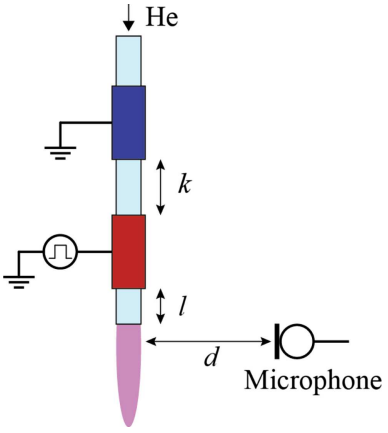

Fig. 1. Experimental set up. High voltage pulses are applied to the powered electrode, which was located at the distance l from the glass tube outlet (distance l was varied from 1 to 20 cm). The grounded electrode was located above the powered electrode, with a separation distance k from 1 to 25 cm. A microphone position relative to the glass tube outlet, d, was between 1 and 15 cm.

(optical fiber), hence it is safe to introduce into plasma, unlike traditional metallic thermocouples. The sensor was loosely inserted into the glass tube, thus we measured the gas temperature not the glass wall. It took several minutes (approximately 10–15 min) for the gas to reach a steady state at high voltages and high frequencies, but the steady-state temperature was reached much faster at lower powers. No noticeable changes were observed in the acoustic measurements over this period. The acoustic measurements were recorded by two calibrated microphones (B&K 4135 and Dayton Audio EMM-6) and a digital sound level meter (BAFX3370). The microphones were positioned perpendicular to the jet flow at a distance between 1 and 15 cm, d in Figure 1.

Ultra-high purity helium (the impurity content <5 ppm in the gas cylinder, Airgas, USA) flowed through the tube at a fixed rate within the range of 1–10 standard liters per minute (slm).

A discharge was ignited in the tube within 1 μs after the HV pulse was applied, and the plume propagated into the open atmosphere, forming a so-called "plasma jet" (Fig. 2a). This apparently continuous plasma jet actually consisted of fast-moving pulses of optical emission (or equivalently a pulse of excitation), which were imaged by an ICCD camera [24,25]. Typically, the emission pulse propagates at speeds around 100 km s^{-1} [26,27], which is much faster than the gas flow rate (up to 10 m s^{-1}) or even the thermal speed of atoms and ions in the plasma. Thus, in this case, differing from fast-moving plasma species, the emission pulse consisted of a fast-moving ionization front caused by a combination of physical events such as Penning ionization, photoionization, and electron acceleration toward the positively charged plasma species, which occurs in the direction opposite to that of the ionization front [28,29]. The discharge in the tube between the electrodes, referred to later in the text as a "plasma core", is a standard dielectric barrier discharge (DBD) with a

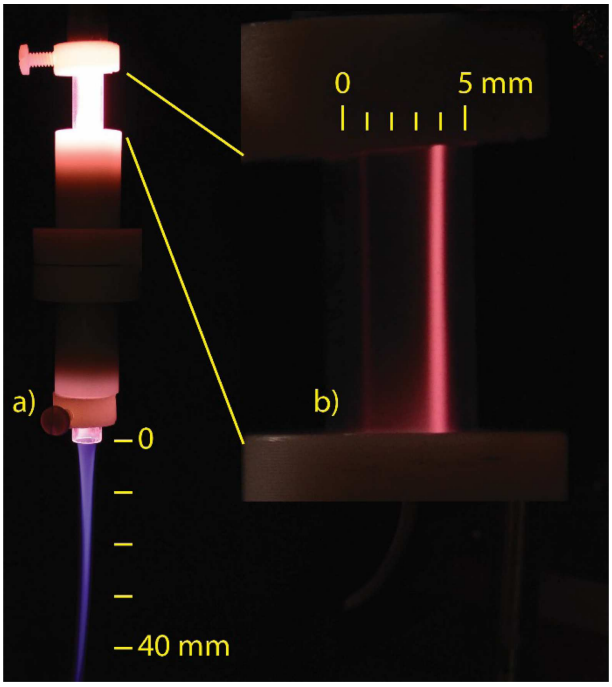

Fig. 2. Photographs of the plasma source taken by a Nikon D3100 camera with an exposure time of 1 s (a) and 1/400 s (b). Plasma source parameters: He flow rate of 6 slm, HV 12 kV pulses with a driving frequency of 1 kHz. Light emission from the plasma core between the electrodes is much stronger than the light emission from the plasma jet region, as is indicated by saturation on the photography with 1 s exposure. To avoid this saturation, the exposure time was decreased 400 times and only then the actual streamer between the electrodes is clearly visible, as shown in (b). However, at this short exposure, the plasma jet is not visible.

streamer [30]. The photographs in Figure 2 show that the light emission from the plasma core region is approximately two orders of magnitude more intense than the emission from the jet, and that was also confirmed by ICCD images (shown later). Such an optical comparison of light emission can suggest that the plasma density, as well as its current and the dissipated electrical power, is also about two orders of magnitude higher in the plasma core. However, a more quantitative analysis should be performed, using specialized techniques.

3 Results and discussion

First, we performed electrical measurements by recording voltage-current characteristics of our APPJ source for different parameters such as voltage, flow rate, driving frequency, pulse duration, and distance between electrodes. The representative electrical measurement shown in Figure 3 was performed by the voltage measurement on the powered electrode and the current measurement on the grounded electrode. A current measurement on the powered electrode displayed a slight difference from that on the grounded electrode, showing a higher (about

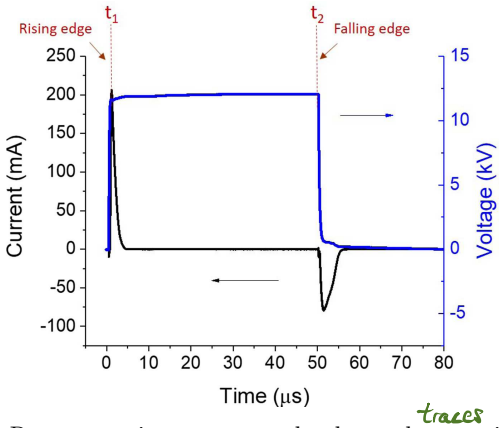

Fig. 3. Representative current and voltage ~~characteristics~~ traces for 12 kV positive voltage pulses with a pulse duration of 50 μs (with times t_1 and t_2 indicating the rising and falling edges, respectively) and a driving frequency of 1 kHz for an He flow rate of 4 slm and the distance between electrodes of 2 cm. The current was measured at the grounded electrode and averaged over one hundred pulses, and the applied voltage was measured at the powered electrode.

10%) electrical noise level. This implies that the current branching from the powered electrode through the plasma jet was significantly smaller, which is in an agreement with the optical measurements. In Figure 3, the current peaks at the beginning of the pulse (i.e., at the rising edge of the pulse) and at the end of the pulse (i.e., at the falling edge of the pulse) showed the DBD behavior of the plasma, which means that the discharge is a self-extinguishing plasma. The charge accumulates on the glass wall, hence the reason for the duration of the discharge being independent of the duration of the applied voltage, with the total charges at the rising and falling edges equal but with an opposite polarity. In time-resolved ICCD images, both plasma discharges ignited at the rising and the falling edges of the pulse showed a propagation of light emission both from the plasma core and the jet regions (Fig. 4). However, the plasma jet intensity was lower in the case of the falling edge. These images show that the plasma ignition occurs on the edge of the powered electrode, where the electrical field is the strongest. Then, plasma propagates outwards from the powered electrode, that is downstream to the open atmosphere to form the jet, and upstream to the grounded electrode to form the plasma core. Both directions of plasma propagation occur regardless of the electrical field direction, which has opposite directions for the rising and the falling edges of the pulse. This is a characteristic of streamers with an ionization front that relies not only on an electron avalanche, but on Penning ionization and photoionization.

Further, we performed acoustic characterization of our APPJ source by using two microphones. The typical acoustic signals for positive and negative voltages are presented in Figure 5. Discharges ignited at the rising and falling edges both generated pressure perturbation that the two microphones each recorded as a sharp dip in the acoustic signal, followed by an overshot, as shown

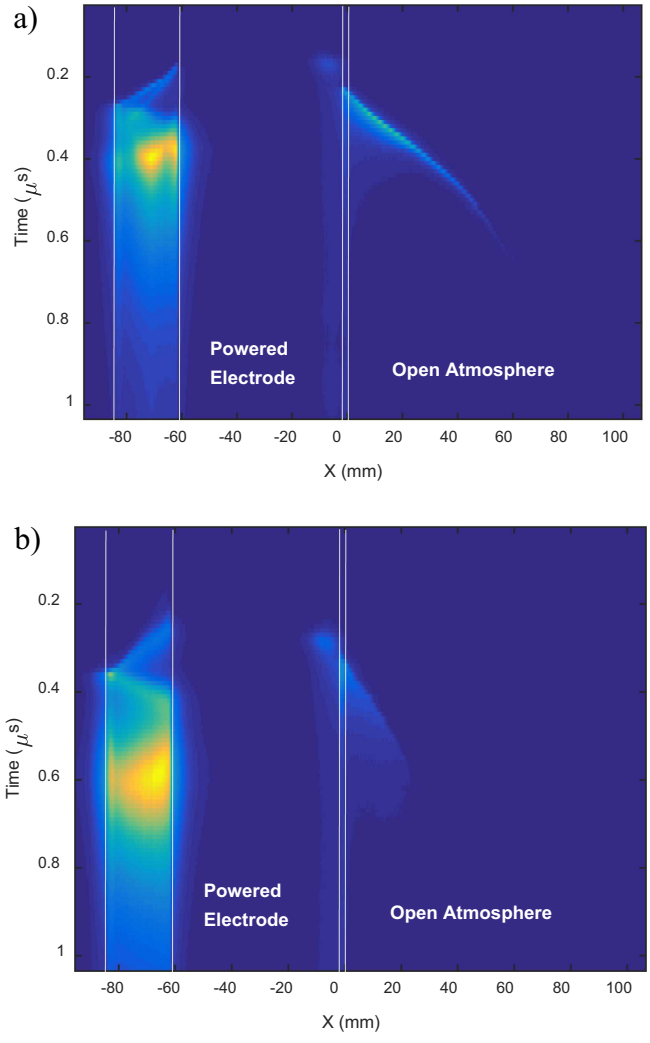

Fig. 4. Propagation of plasma between the electrodes and into the open atmosphere during the first 1 μs of the applied 12 kV pulse for the rising edge (a) and during the first 1 μs after the pulse for the falling edge (b) for an He flow rate of 4 slm. The horizontal axis represents a position along the tube with the zero at the tube outlet, and the vertical axis represents time (increasing downwards).

in Figure 5. There was a slight difference in the shape of the dips for plasma pulses for the rising and falling edges. The dip had more fluctuations at the beginning of the perturbation for the rising edge, with more fluctuations occurring at the end for the falling edge. In the case of negative voltage pulses, the fluctuations observed for the dip were reversed at the rising and falling pulse edges. In other words, the fluctuations were detected at the beginning for the falling edge and at the end for the rising edge. The absolute value of dip and overshot of the acoustic signal (later referred to as "a peak to peak amplitude") depended on the voltage applied and the distance between the microphone and jet, and it corresponded to approximately 0.1 Pa or 85 dBA at a distance of 10 cm for 12 kV pulses.

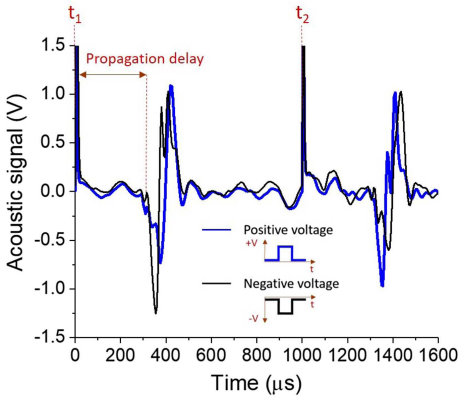

Fig. 5. Acoustic waveforms for 10 kV positive and negative voltage applied to the powered electrode for pulses of 1 ms duration with a driving frequency of 200 Hz and for an He flow rate of 4 slm. The distance between the electrodes (k) was 3 cm, the distance between the powered electrode and the tube outlet (l) was 1 cm, and the distance to the microphone (d) was 10 cm. The sharp peaks at 0 (t_1) and 1000 μs (t_2) were caused by electrical noise at the rising and falling edges of the pulse. Here, an acoustic signal, i.e., pressure perturbation, is presented as an electrical signal read from a microphone.

As seen in Figure 5, the acoustic signal was delayed several hundred microseconds after the plasma ignition. This time delay is due to the speed of the sound propagation to the microphone. We recorded acoustic waveforms for several distances between the microphone and the tube outlet, from which we obtained the propagation delay between the rising edge or the falling edge of the pulse and changes in pressure. In Figure 6, the dependence of propagation delay as a function of the microphone distance is presented for the pulse duration of 500 μs. Both curves show the linear dependence with a relative shift of 500 μs in time delay demonstrated for the rising and falling edges, which corresponds to the duration of the applied pulse. A linear fit showed that the speed of the sound propagation was 347 ($\pm$5) m s^{-1}, as expected for the sound propagation in air at room temperature. In Figure 6, the extrapolation to zero distance (not shown in the figure) between the microphone and the tube outlet yielded a time delay of 90 ($\pm$3) μs after the rising edge of the pulse and 66 ($\pm$3) μs after the falling edge of the pulse. This indicated that the sound did not originate at the outlet of the glass tube or in the plasma jet, but rather inside the glass tube.

We also performed another time-delay measurement, in which the microphone distance was fixed and the distance of both electrodes from the tube outlet varied (Fig. 7). For these particular experimental parameters, the sound propagated in the glass tube at a speed of 960 ($\pm$20) m s^{-1}, which corresponds to the speed of sound in helium at room temperature, as calculated from Figure 7.

By extrapolating the data and taking into account the velocities of the sound propagation in Figures 6 and 7, it was possible to estimate the location of the sound generation. For instance, for an electrode separation of 3 cm, the sound was generated between both electrodes. More

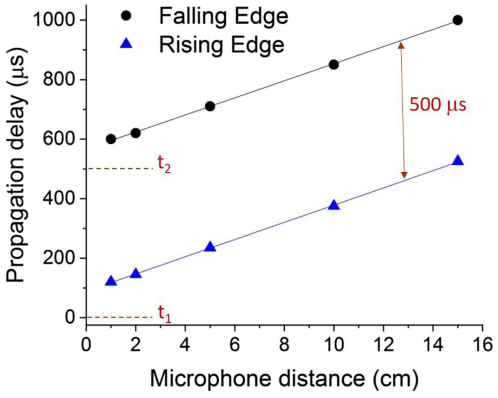

Fig. 6. Propagation delay of the acoustic signal after plasma ignition as a function of the distance between the microphone and the tube outlet (d in Fig. 1) for plasma ignited at the rising (t_1) and falling (t_2) edges. The time delay was obtained from acoustic waveforms for 10 kV positive voltage applied to the powered electrode for pulses of 500 μs duration, with a driving frequency of 1 kHz and for an He flow rate of 2 slm. The distance between the electrodes (k) was 3 cm, and the distance between the powered electrode and the tube outlet (l) was 1 cm.

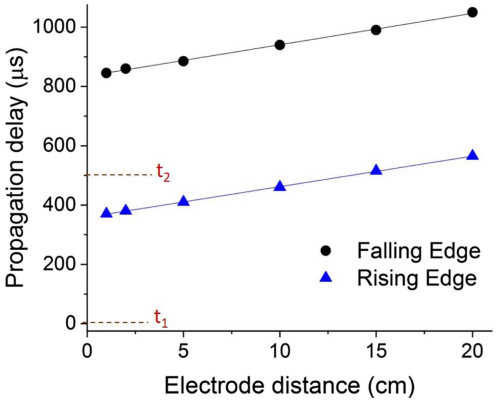

Fig. 7. Propagation delay of the acoustic signal after plasma ignition as a function of the powered electrode distance from the tube outlet (l in Fig. 1). The time delay was obtained from acoustic waveforms for 10 kV positive voltage applied to the powered electrode for pulses of 500 μs duration, with a driving frequency of 1 kHz for an He flow rate of 2 slm. The distance between the electrodes (k) was 3 cm and the distance to the microphone (d) was 10 cm.

precisely, the sound origin for the rising pulse edge was estimated to be located approximately 2 cm from the powered electrode and 1 cm from the grounded electrode, while for the falling discharge the sound origin was on the edge of the powered electrode. Hence, the sound was generated by the streamer between the electrodes, and not by the plasma jet.

Additional evidence that the streamer in the plasma core generated the sound, rather than the jet, was obtained by changing the separation distance between both electrodes. In this experiment, we fixed the distance of the powered electrode at 1 cm from the glass tube

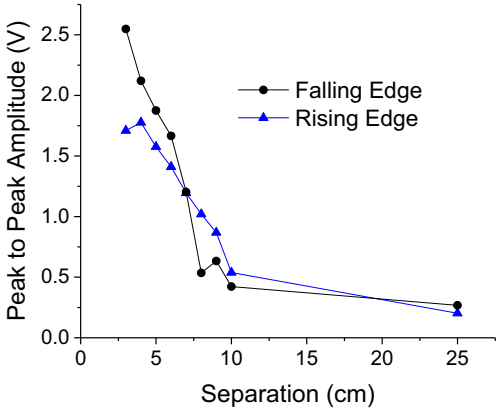

Fig. 8. Dependence of pressure perturbations as a function of the separation between the electrodes (k in Fig. 1). The peak-to-peak amplitude was obtained from acoustic waveforms for 10 kV positive voltage applied to the powered electrode for pulses of 500 μs duration, with a driving frequency of 100 Hz and for an He flow rate of 2 slm. The distance between the powered electrode and the tube outlet (l) was 1 cm and the distance to the microphone (d) was 10 cm.

outlet, and we varied the distance between the electrodes by moving the grounded electrode farther from the powered electrode. Figure 8 presents the peak-to-peak amplitudes read from the acoustic waveforms as a function of the separation between both electrodes from 3 to 25 cm for both the rising and the falling pulse edges. This figure shows that the sound intensity decreased rapidly as the separation distance between the electrodes increased, which is consistent with the decreased intensity of light emission in the plasma core under the same conditions. This quenching of light emission is due to a weaker applied electrical field created when the distance between the electrodes is increased while the applied voltage is kept constant. Nevertheless, the light emission in the plasma jet remained relatively constant, because the electrical field in the region of the plasma jet remains unchanged, even for larger separations between electrodes.

The fact that acoustic waveforms for both rising and falling edges and both positive and negative voltages showed similarities, i.e., first a dip in the signal, which is followed by an overshoot, as seen in Figure 5, indicates that the sound is unlikely to have been caused by electrodynamical coupling of the applied electrical field and electrically charged particles in the plasma. If the sound was generated by the ions accelerated in the applied electrical field, the shape of acoustic waveforms for the positive and negative voltages should be reversed. In other words, in one case the dip would precede the overshoot, and in the other case it would be opposite, which is not the data that we recorded. We propose that, rather than being due to the electrodynamical coupling, the sound is caused by a rapid thermal expansion of the gas during the discharge between electrodes. Furthermore, we can assume that a similar amount of electrical energy is pumped into the system for both discharges ignited at the rising and falling edges, and for both cases of positive and negative

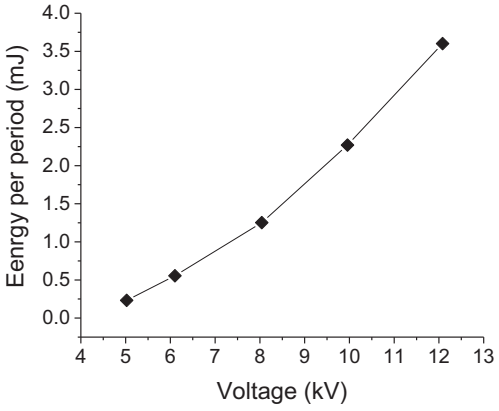

Fig. 9. Energy pumped into the system per one period as a function of the applied voltage. The energy pumped to the system was calculated as the integral of the product of the voltage applied and the current measured at the grounded electrode during one period. Because this energy was calculated for one period, half of this amount is consumed and dissipated during plasma ignition, either at the rising or the falling pulse edges.

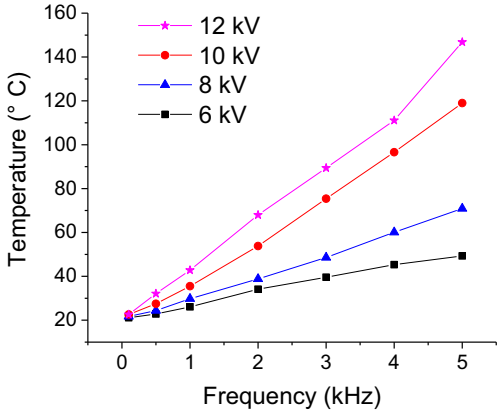

Fig. 10. Gas temperature of the plasma core as a function of the driving frequency with a constant duty cycle of 50% for several applied voltages after reaching a local equilibrium with the glass tube (about 5 min after plasma ignition) with an He flow rate of 2 slm. The distance between the electrodes (k) was 2 cm, and the distance between the powered electrode and the tube outlet (l) was 1 cm.

voltage applied. In all of these cases, the pumped energy rapidly heats the gas, causing the local pressure perturbation as observed in the acoustic waveforms (Fig. 5). We also calculated the total energy pumped into the system per period from the current and the voltage characteristics (Fig. 3). From these calculations, we plotted the dependence of the energy pumped as a function of the applied voltage (Fig. 9). As seen in Figure 9, this energy is within the range of a few mJ. Moreover, this energy is almost entirely pumped into the plasma core region as a heat, and with helium being a very good heat conductor, it is transferred quickly to the glass tube and the electrodes until the gas temperature reaches a local equilibrium with the glass tube.

Therefore, we measured gas temperature in the plasma core region and plasma jet using a fiber optic temperature sensor. There are several parameters which affect the gas temperature, such as flow rate, APPJ source geometry, and the average power pumped into the system. Because the average power pumped into the system is a product of the energy per one pulse and the driving frequency, we measured the gas temperature in the plasma core as a function of driving frequency for several applied voltages (Fig. 10). As seen in Figure 10, the gas temperature in the plasma core can reach up to 160 °C for the applied voltage of 12 kV and driving frequency of 5 kHz. At these conditions, the plasma jet temperature was ∼120 °C. We found that for the applied voltages below 10 kV and frequencies below 1 kHz, the plasma jet is close to room temperature, which is an important consideration for medical applications.

As shown in Figure 3, the power is pumped into the system only during a brief time of plasma discharge (shorter than 10 μs) at the rising and falling pulse edges of each pulse. Therefore, it can be expected that, during this short time, the local gas temperature will briefly increase before reaching equilibrium with the glass tube. However, our temperature measurements were not fast enough to record such a brief increase in temperature. We were only able to record the temperature changes within 1 s, which was the shortest acquisition time in our experiment. In order to estimate the maximum temperature increase, we assumed that the entire energy is temporarily converted into heat, which was used to warm up the mass of helium gas (0.35 mg) in the tube with a length of 10 cm and an inner diameter of 5 mm. We neglected the gas flow and assumed the stationary case, because the time scale for plasma ignition and abrupt heat of the gas is much shorter than the flow rate of the mass. The energy per period plotted in Figure 9 was divided into two discharges formed at the rising and the falling edges, which is about 1.5 mJ per discharge for a 12 kV pulse. The helium heat capacity is 5.19 J g^{-1} K^{-1} [31]; therefore, a brief increase in temperature for a 12 kV discharge is about 0.8 K, or smaller than 0.3% of the average gas temperature after reaching equilibrium in Figure 10.

Although this is a small change in gas temperature, an equivalent sound pressure level (SPL) can be determined. Analysis by Mazzolla and Molen [12] is based on an adiabatic assumption and small modulation depth of a DC glow plasma discharge so that

$$\frac{\delta p}{p} = \frac{\gamma}{\gamma - 1}\frac{\delta T}{T}$$

where p is the ambient pressure, δp is the pressure change, T is the steady-state temperature, δT is the temperature change and γ is the heat capacity ratio for helium (1.66 at 293 K). Using ambient pressure of one atmosphere (101 kPa) and a steady state temperature of 433 K, a temperature change of 0.8 K corresponds to a pressure change of ±469 Pa. An SPL can be calculated from

$$\mathrm{SPL} = 20\,\mathrm{Log}\frac{P_e}{P_{\mathrm{ref}}}$$

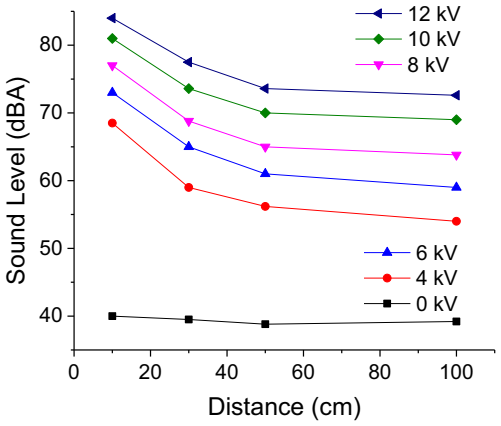

Fig. 11. Sound level as a function of the distance from the plasma jet and for positive voltages between 0 (just He flow) and 12 kV for pulses with 500 μs duration and a driving frequency of 1 kHz and for an He flow rate of 4 slm. The distance between the electrodes (k) was 3 cm, and the distance between the powered electrode and the tube outlet (l) was 1 cm.

where P_{ref} is a reference root mean squared pressure level taken as the threshold of human hearing (20 μPa) In this example, the SPL exceeds 140 dB and, at 5 kHz modulation, the SPL would not differ significantly when an A-weighting correction is applied. The calculated SPL above differs significantly from that measured (see Fig. 11) even when a correction is applied for the microphone/plasma jet separation and is likely due to the plasma operating under non-adiabatic conditions, where at low kHz frequency modulation, thermal conduction becomes significant when compared to the timescales required for heat to be ~~input~~ into the discharge. A fuller understanding of the SPL and its relation to temperature changes would require an improved model which is outside the scope of this work.

From the perspective of medical applications, as mentioned above, it is important to characterize APPJ sources regarding ~~their variety of~~ safety ~~aspects~~. Therefore, we conducted studies on a sound level detected from our APPJ source. The sound level was measured by a digital sound level meter for applied voltages between 4 and 12 kV, and a driving frequency of 1 kHz, at distances of 10–100 cm from the plasma jet. The results are shown in Figure 11. The plot shows that decrease in the SPL is inversely proportional to the distance from the source and is characteristic of a point source. The sound levels recorded were below 85 dBA, which is the limit for the safe exposure over 8 h, recommended by the National Institute for Occupational Safety and Health [14]; hence, the plasma jet source used in this research does not represent a hazardous source of noise for the patient and physician with a normal exposure up to 8 h.

It is relevant to note that in our previous studies on the biological effects of APPJ on biomolecular targets, which were performed using the same plasma source and the same electrical conditions, we observed damage to DNA [32,33]. Thus, it indicates that the source that can be operated at the safety sound level is capable of producing the plasma components that can induce alternation to the cellular components.

4 Conclusion

We performed a series of systematic acoustic, electrical, thermal, and optical emission studies by varying different experimental parameters. In conclusion, from a fundamental point of view, our results demonstrated that the sound is generated in the plasma core region between the electrodes, and not within the jet, which launches into the open atmosphere. We suggest that within a brief time (~1 μs), the discharge between the electrodes forms a streamer that abruptly heats ~~a~~ gas. ~~Afterwards~~, The gas expands quickly, causing ~~a~~ pressure perturbations, which propagate ~~s~~along the glass tube, forming an acoustic ~~wave~~. From an application point of view, the sound levels, coming from the APPJ source, were within recommended levels. However, the sound intensity could be lowered, if necessary, by reducing the intensity of the plasma between the electrodes, without affecting the plasma jet itself significantly in respect to its temperature. Practically, this could be accomplished by increasing the separation distance between the electrodes, or even removing the grounded electrode completely. The results and findings obtained in this work contribute to a deeper understanding of the physical processes accompanied by an atmospheric pressure plasma discharge, and provide useful information that is essential for clinical approvals of plasma technology in a number of medical applications.

The authors would like to thank Yaoyi Guan and Scott C. Morris for their help in preliminary acoustic measurements. This material is based upon work supported by the U.S. Department of Energy Office of Science, Office of Basic Energy Sciences under Award Number DE-FC02-04ER15533. This is contribution number NDRL 5279 from the Notre Dame Radiation Laboratory.

Author contribution statement

All the authors were involved in the preparation of the manuscript. All the authors have read and approved the final manuscript.

Publisher's Note The EPJ Publishers remain neutral with regard to jurisdictional claims in published maps and institutional affiliations.

References

1. A. Schutze, J.Y. Jeong, S.E. Babayan, J. Park, G.S. Selwyn, R.F. Hicks, **26**, 1685 (1998)
2. J.Y. Jeong, S.E. Babayan, V.J. Tu, J. Park, I. Henins, R.F. Hicks, G.S. Selwyn, Plasma Sources Sci. Technol. **7**, 282 (1999)
3. X. Dai, K. Bazaka, D.J. Richard, E.W. Thompson, K. Ostrikov, Trends Biotechnol. **36**, 1183 (2018)

4. M. Schuster, C. Seebauer, R. Rutkowski, A. Hauschild, F. Podmelle, C. Metelmann, B. Metelmann, T. von Woedtke, S. Hasse, K.-D. Weltmann, H.-R. Metelmann, J. Cranio-Maxillofacial Surg. **44**, 1445 (2016)
5. X. Lu, G.V. Naidis, M. Laroussi, S. Reuter, D.B. Graves, K. Ostrikov, Phys. Rep. **630**, 1 (2016)
6. S. Reuter, T. von Woedtke, K.-D. Weltmann, J. Phys. D: App. Phys. **51**, 233001 (2018)
7. K.P. Arjunan, V.K. Sharma, S. Ptasinska, Int. J. Mol. Sci. **16**, 2971 (2015)
8. W. Duddell, Nature **63**, 182 (1900)
9. G. Shirley, J. Audio Eng. Soc. **5**, 23 (1957)
10. M.K. Lim, Appl. Acoust. **14**, 245 (1981)
11. P. Bequin, P. Herzog, Acustica **83**, 359 (1997)
12. M.S. Mazzolla, G.M. Molen, J. Acoust. Soc. Am. **81**, 1972 (1987)
13. D.M. Tombs, Nature **176**, 923 (1955)
14. J.R. Franks, M.R. Stephenson, C.J. Merry, *Preventing Occupational Hearing Loss: A Practical Guide* (US Department of Health and Human Services, Public Health Service, Centers for Disease Control and Prevention, National Institute for Occupational Safety and Health, Division of Biomedical and Behavioral Science, Physical Agents Effects Branch, 1996)
15. F. Bastien, J. Phys. D. Appl. Phys. **20**, 1547 (1987)
16. Y. Sutton, J. Moore, D. Sharp, N.S.J. Braithwaite, IEEE Trans. Plasma Sci. **39**, 2146 (2011)
17. F. Mitsugi, IEEE Trans. Plasma Sci. **47**, 4781 (2019)
18. J. Winter, R. Brandenburg, K.-D. Weltmann, Plasma Sources Sci. Technol. **24**, 64001 (2015)
19. E. Robert, V. Sarron, D. Riès, S. Dozias, M. Vandamme, J.-M. Pouvesle, Plasma Sources Sci. Technol. **21**, 34017 (2012)
20. X. Lu, M. Laroussi, V. Puech, Plasma Sources Sci. Technol. **21**, 34005 (2012)
21. X. Han, W.A. Cantrell, E.E. Escobar, S. Ptasinska, Eur. Phys. J. D **68**, 46 (2014)
22. E. Adhikari, S. Ptasinska, Eur. Phys. J. D **70**, 180 (2016)
23. U. Roland, C. Renschen, D. Lippik, F. Stallmach, F. Holzer, Sens. Lett. **1**, 93 (2003)
24. D. Maletić, N. Puač, N. Selaković, S. Lazović, G. Malović, A. Dordević, Z.L. Petrović, Plasma Sources Sci. Technol. **24**, 25006 (2015)
25. D. Dobrynin, A.A. Fridman, Plasma Med. **8**, 177 (2018)
26. D. Breden, K. Miki, L.L. Raja, Appl. Phys. Lett. **99**, 2009 (2011)
27. S. Park, S. Youn Moon, W. Choe, Appl. Phys. Lett. **103**, (2013)
28. R. Wang, K. Zhang, Y. Shen, C. Zhang, W. Zhu, T. Shao, Plasma Sources Sci. Technol. **25**, 15020 (2016)
29. W. Liu, Z. Li, L. Zhao, Q. Zheng, C. Ma, Phys. Plasmas **25**, 083505 (2018)
30. A. Chirokov, A. Gutsol, A. Fridman, Pure Appl. Chem. **77**, 487 (2005)
31. S. Hwang, W.R. Weltmer, in *Kirk-Othmer Encycl. Chem. Technol.* (John Wiley & Sons, Inc., Hoboken, NJ, USA, 2000)
32. E.R. Adhikari, V. Samara, S. Ptasinska, J. Phys. D **51**, 185202 (2018)
33. E.R. Adhikari, V. Samara, S. Ptasinska, Biol. Chem. **400**, 93 (2019)